Strongly frustrated magnetism and colossal magnetoresistance in polycrystalline $La_{0.47}Ce_{0.20}Ca_{0.33}MnO_3$

G. Alejandro*
Centro Atómico Bariloche, CNEA, Av. Bustillo 9500, (8400) San Carlos de Bariloche, Río Negro, Argentina

D. G. Lamas
CINSO (Centro de Investigaciones en Solidos), CITEFA-CONICET, J. B. de La Salle 4397, (1603) Villa Martelli, Pcia. de Buenos Aires, Argentina

L. B. Steren, J. E. Gayone,† G. Zampieri,‡ A. Caneiro, M. T. Causa, and M. Tovar
Centro Atómico Bariloche, CNEA, Av. Bustillo 9500, (8400) San Carlos de Bariloche, Río Negro, Argentina
(Received 4 October 2002; revised manuscript received 17 December 2002; published 28 February 2003)

We present x-ray diffraction, x-ray photoemission spectroscopy, magnetization, and transport results on the cerium-doped manganite $La_{0.47}Ce_{0.20}Ca_{0.33}MnO_3$. We have achieved good quality, single-phase polycrystalline samples by the nitrate decomposition route. A Rietveld analysis of the x-ray spectrum revealed a distorted structure with a small Mn-O-Mn apical angle of 152.6°. We found that both $3+$ and $4+$ charge states of cerium ions coexist, introducing an additional source of cation disorder in the *A* site of the perovskite structure. The low-temperature magnetization measurements, together with the high-T susceptibility results, indicate a magnetically frustrated behavior below $T_F \approx 70$ K. The zero-field resistivity shows, at $T_M \approx 145$ K, the typical metal-insulator transition found in manganite systems, though a temperature for a long-range ferromagnetic order transition does not obviously exist. The magnetoresistance (MR) is large, with a maximum value close to 100%. Strong hysteresis effects are observed in the MR vs field curves, that correlate well with the magnetization vs temperature measurements. We discuss these observations and show that the resistivity results are closely related to the magnetic behavior of the system.

DOI: 10.1103/PhysRevB.67.064424 PACS number(s): 75.47.Gk, 71.30.+h

I. INTRODUCTION

In manganite systems $La_{1-y}D_yMnO_3$ (D=Ca, Sr, Ba), with a perovskite structure ABO_3, the double-exchange mechanism,[1] responsible for the ferromagnetism and metallic conductivity of these compounds, is optimized for doping levels $y \approx 1/3$. At these concentrations, the largest values of colossal magnetoresistance (CMR) are also obtained.

When the lanthanum in the *A* site of the perovskite is partially replaced by yttrium or a rare-earth such as Pr or Tb, the cation disorder introduced in the structure has been shown to lead to different and interesting phenomena, depending on the nature of the substitute cation. Magnetic frustration has been observed[2–4] in $La_{0.67-x}Y_xCa_{0.33}MnO_3$, spin glass behavior was reported[5] in $La_{0.7}Tb_{0.3}Ca_{0.33}MnO_3$, and evidence of electronic phase separation was found[6] in $La_{5/8}Pr_{3/8}Ca_{1/3}MnO_3$.

The average ionic radius of the *A* site seems to play an important role, through the tolerance factor of the structure. Isovalent substitutions, such as those with Y or Pr, have been widely investigated, but nonisovalent substitutions have only recently attracted some attention.[7–11]

Why do the (La, Pr)Ca compounds show evidence of electronic phase separation while the magnetic behavior of (La, Y)Ca and (La, Tb)Ca seems to be closer to a spin glass? Is the bending of the Mn-O-Mn angles, produced by the chemical pressure induced by the mismatch of different ionic radii in the *A* site, the only relevant parameter? These questions led us to prepare and characterize polycrystalline samples of (La, Ce)Ca with an *a priori nominal hole concentration* of 33%. On the one hand, doping values close to 0.33 are known to maximize the CMR in other manganite systems; on the other hand, this choice will allow us to compare our results with different studies reported in the literature on yttrium and rare-earth (Pr, Tb) substituted samples with nominal hole doping values close to 1/3.

In cerium-doped manganites, it is possible for Ce^{3+} and Ce^{4+} species to coexist in the same compound, adding an extra source of structural disorder. Today, the experimental data on cerium-doped manganites available in the literature are limited,[7–11] and not conclusive in various aspects. In particular, the question about the valence state of Ce ions in these compounds is still an open matter. In a previous work by Kang *et al.*,[11] where x-ray photoemission spectroscopy (XPS) measurements on polycrystalline $La_{0.7}Ce_{0.3}MnO_3$ were reported, the authors claimed that the charge state of cerium ions is mainly $4+$, although the coexistence of both valences states should not be discarded. In an attempt to shed some light on these open questions, we report on x-ray powder diffraction (XRD), XPS, magnetization, and magnetotransport results obtained in very good quality samples of polycrystalline, single-phase $La_{0.47}Ce_{0.20}Ca_{0.33}MnO_3$.

II. EXPERIMENTAL DETAILS

Powder samples of $La_{0.47}Ce_{0.20}Ca_{0.33}MnO_3$ were prepared using the nitrate decomposition route, and final calcination treatments were done at 1450 °C for 3 h. The incorporation of cerium cations in the perovskite lattice was monitored by

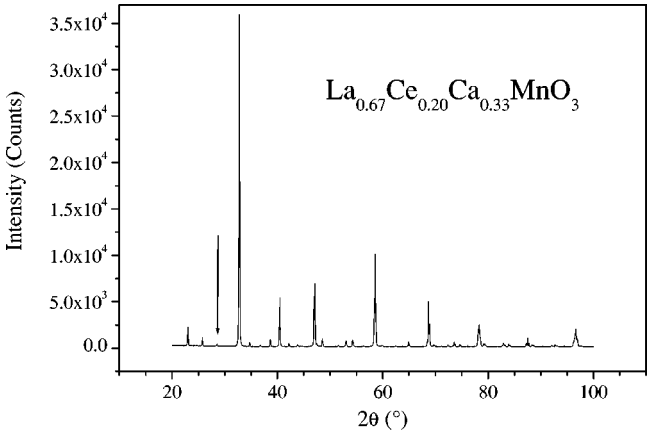

FIG. 1. Powder diffractogram of polycrystalline $La_{0.47}Ce_{0.20}Ca_{0.33}MnO_3$ at RT. It corresponds to a *Pnma* perovskite structure. The arrow points to the (111) reflection of CeO_2; a Rietveld-based estimation indicates only 0.6 wt. % of segregated cerium oxide (see text).

powder XRD. Cell parameters, Mn-O distances, and Mn-O-Mn bond angles were determined by a Rietveld analysis using the program FULLPROF.[12]

The valence state of cerium ions was investigated through XPS measurements. The experiments were performed at room temperature (RT), and the spectra were collected using an incident photon energy of $h\nu = 1486.6$ eV.

Magnetization measurements were performed in a superconducting quantum interferece device magnetometer from 5 to 300 K, and magnetic fields up to 50 kOe. High-temperature magnetization experiments were carried out in a Faraday balance magnetometer in the temperature range 300–1000 K. Magnetotransport measurements were done in a standard four-probe geometry, under magnetic fields up to 50 kOe, and temperatures between 4 and 300 K.

III. RESULTS AND DISCUSSION

A. Sample characterization

1. Powder x-ray diffraction

Preparing good quality samples of cerium-doped manganites is a difficult task. The high quality of the $La_{0.47}Ce_{0.20}Ca_{0.33}MnO_3$ powder obtained in this work is reflected in the x-ray diffraction spectrum shown in Fig. 1, where only the characteristic perovskite peaks have strong intensities. From the very low intensity of the CeO_2 peak at 28° we estimate that less than 0.6 wt. % of cerium oxide is segregated, i.e., only 3.6% of cerium ions are out of the perovskite compound.

Our result differs from some previous reports[7,8] on $La_{1-x}Ce_xMnO_3$ samples, where intense CeO_2 peaks appeared in the x-ray spectra, reflecting an important segregation of cerium oxide. The routes employed to prepare those bulk polycrystalline samples included wet methods[7] and solid state reaction.[8] In the x-ray spectra of the samples reported in Refs. 7 and 8, unreacted cerium oxide is signaled by the presence of the 28°, 47°, and 56° peaks, characteristic of CeO_2. Ganguly *et al.*[13] demonstrated, after preparing samples of $La_{1-x}Ce_xMnO_3$ by the solid state reaction route and performing careful x-ray diffraction experiments, that the samples so obtained were not single phased. On the contrary, they were actually multiphase mixtures comprising hole-doped lanthanum-deficient manganite phases, and cerium oxide CeO_2. Although the reasons for CeO_2 segregation in those samples[7,8,13] are not well established, it may be related to the presence of Ce^{4+} cations. For air-prepared samples, the most stable valence state of cerium is expected to be $4+$. Therefore, charge neutralization would require the formation of Mn^{2+}. On the one hand, Mn^{2+} is a much larger cation that Mn^{3+} and Mn^{4+}; on the other hand, Ce^{4+} is a much smaller ion than La^{3+} or Ce^{3+}. Both effects led to a very low tolerance factor,[14] whose value is 0.907 for all cerium ions in the $4+$ charge state in $La_{2/3}Ce_{1/3}MnO_3$. This fact indicates that the cerium-doped structure is very unstable and, as a consequence, CeO_2 segregation would occur.

In our calcium-doped compound $La_{0.47}Ce_{0.20}Ca_{0.33}MnO_3$, however, the presence of Ca^{2+} stabilizes the structure by allowing the substitution with tetravalent cerium ions without requiring the formation of Mn^{2+}. In this system, the tolerance factor would rise to 0.950, if all cerium ions were in the $4+$ state. Under these more favorable structural conditions, cerium was accepted by the structure by annealings at 1450 °C. Therefore, our samples are essentially single phased. At RT, we determined an orthorhombic (*Pnma*) structure with parameters $a = 5.4824(4)$ Å, $b = 7.7184(4)$ Å, and $c = 5.4610(4)$ Å. The Mn-O-Mn distances are $s = 1.8355(4)$ Å, $m = 1.9862(4)$ Å, and $l = 2.0896(4)$ Å, and the two Mn-O-Mn angles are 152.6° (5) for apical O(1), and 160.6° (5) for equatorial O(2).

The average value of the three Mn-O-Mn bond angles observed in manganites vary approximately[3,15] from 156.5° to 168.5°. In the $La_{0.67-x}Y_xCa_{0.33}MnO_3$ series, average angles of 159.7°, 158.3° and 157.6° have been reported for $x = 0.05$, 0.15, and 0.20 respectively.[3,4] In this context, our experimental value of 157.9° is not unusual. However, it is interesting to note that the *difference* between apical and average bond angles are larger in $La_{0.47}Ce_{0.20}Ca_{0.33}MnO_3$. Indeed, while in the (La, Y) series[16,17] this difference is less than 1%, in our cerium-doped compound it rises to 3%.

2. X-ray photoemission spectroscopy

Figure 2 shows the XPS spectrum of $La_{0.47}Ce_{0.20}Ca_{0.33}MnO_3$ in the region of the Ce-3d core-level peaks. Three structures labeled *A*, *B*, and *C* are clearly visible in the spectrum centered at about 917, 900, and 884 eV, respectively. To help in the identification of these structures we have also included in the figure the spectra of CeO_2 and Ce_2O_3 (taken from Ref. 18), representative of Ce ions in the $+4$ and $+3$ charge states, respectively. Each one of these spectra is composed of two identical multiplets shifted by 18.5 eV, with relative intensities 3:2, that correspond to the spin-orbit-split $3d_{5/2}$ and $3d_{3/2}$ core holes. The different multiplets in CeO_2 and Ce_2O_3 reflect their different $4f$ occupations in the ground states. It can be seen in Fig. 2 that the structure labeled *C* in the spectrum of $La_{0.47}Ce_{0.20}Ca_{0.33}MnO_3$ is contributed to by the peaks V'' and

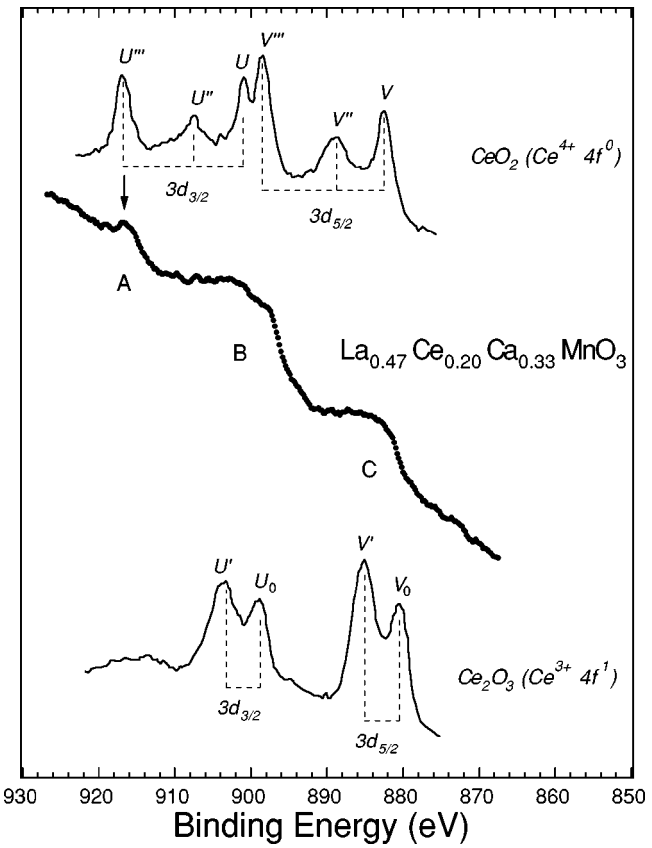

FIG. 2. XPS spectrum of $La_{0.47}Ce_{0.20}Ca_{0.33}MnO_3$ in the region of the Ce-3*d* core-level peaks. Also included for comparison are the spectra of CeO_2 and Ce_2O_3 (thin solid lines) taken from Ref. 18.

V of the CeO_2 spectrum and by the peaks V' and V_0 of the Ce_2O_3 spectrum. Similarly, the broad structure labeled B gets contributions from the peaks U'', *U*, and V''' of the CeO_2 spectrum and from the peaks U' and U_0 of the Ce_2O_3 spectrum. In this case, however, there is an additional contribution coming from the $L_3M_{2,3}V$ Auger electrons of Mn, which have kinetic energies in the range 575–594 eV, and thus apparent binding energies in the range 893–908 eV. Finally, it is seen that the peak labeled A coincides in shape and position with the peak U''' of the CeO_2 spectrum, and is, therefore, a clear indication of the presence of Ce^{4+} ions in the compound. From the intensity of this peak one can estimate the intensities of the V'' and *V* contributions to the structure *C* and by difference the intensities of the V' and V_0 contributions. The relative intensities of the contributions (V'',V) and (V',V_0) give the percentages of Ce ions in the $+4$ and $+3$ charge states, respectively. Our conclusion is that about 60% of the cerium atoms are in the $+4$ charge state and the remaining 40% in the $+3$ charge state. This result indicates that our samples are hole-doped compounds with an effective level of 21%. Future studies with careful control of oxygen stoichiometry are encouraged to determine the Mn valence state in these cerium-doped manganites.

B. High-temperature susceptibility

The high-temperature dc magnetization is linear with the magnetic field up to $H=50$ kOe above $T\approx 200$ K. The inverse of the susceptibility $\chi^{-1}=H/M$ vs temperature, is plotted in Fig. 3 for $T\gtrsim 300$ K. We have made the necessary corrections due to diamagnetic contributions and to the magnetization of cerium ions. Therefore, the curve shown in the figure represents the net Mn ions contribution to the susceptibility. In order to subtract the cerium contribution we assumed that Ce^{3+} and Ce^{4+} ions are present in the relative concentrations estimated from XPS results. Tetravalent cerium has a zero magnetic moment, so we must only subtract the nonzero $Ce^{3+}(\mu_{eff}=2.54\mu_B)$ component. For that purpose we supposed that Ce^{3+} ions are paramagnetic and their magnetization follows a pure Curie law (C_{Ce}/T) in the whole temperature range. This procedure neglects any magnetic coupling between the Ce moments and the surrounding ions. These interactions may be present according to recent neutron diffraction data obtained in $La_{0.7}(Ca_{0.5}Ce_{0.5})_{0.3}MnO_3$ by Wu *et al.*[19] However, the correction introduced to the high temperature susceptibility by subtracting a Curie-Weiss (CW) law[19] with $\Theta_{Ce}\approx 45$ K, instead of a Curie law, is very small, and does not affect our main conclusions.

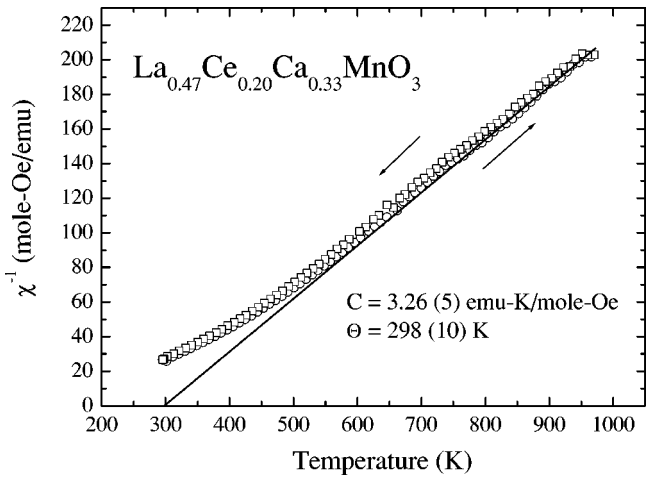

FIG. 3. Inverse of the susceptibility, χ^{-1} vs temperature (on heating: circles; on cooling: squares). The solid line is a CW law fitting with $C=3.26$ (5) emu K/mole Oe, and $\Theta=298$ (10) K.

There is a positive curvature of $\chi^{-1}(T)$ vs *T* at the lower temperatures, which is typical of other manganite systems[20,21] and has been explained in terms of short-range order effects. A subtle anomaly appears close to $T=720$ K, probably associated with the high temperature orthorhombic to rhombohedral transition observed in other lanthanum manganites.[21] Future high-temperature x-ray-diffraction studies are necessary to test this assignment. Well above this feature, χ^{-1} exhibits a CW behavior given by $\chi(T)=C/(T-\Theta)$, with $C=3.26$ (5) emu K/mole Oe $(\mu_{eff}=5.12\mu_B)$, and $\Theta=298$ (10) K. The *C* value so obtained should be compared with the average calculated on the basis of the relative amounts of Ce^{3+} and Ce^{4+} estimated from XPS results, i.e., $C=2.76$ emu K/mole Oe.

An oxygen deficiency, leading to an increment of Mn^{3+} ions, would raise the value of the effective moment. However, the Curie constant corresponding to an oxygen deficient compound with all Mn ions in the $3+$ state is 3.0 emu K/mole Oe. Thus, the observed enhancement of the

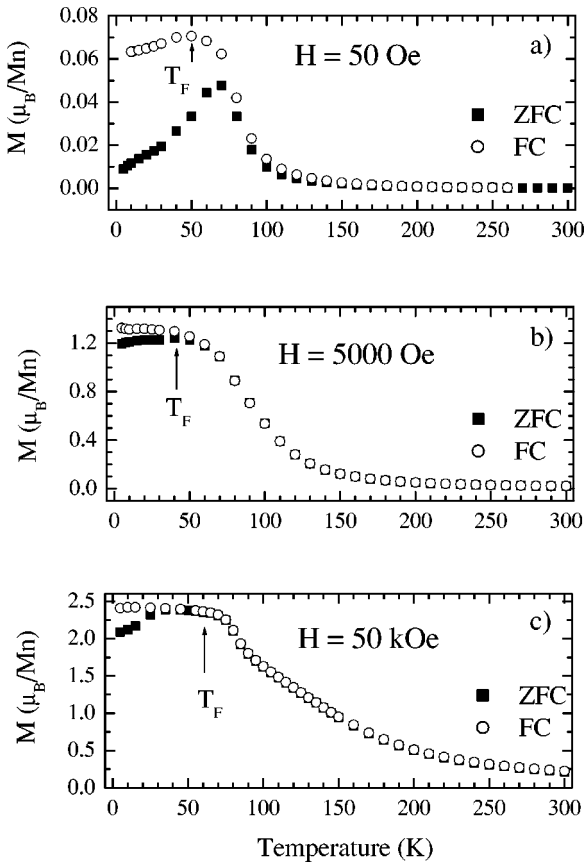

FIG. 4. Zero-field-cooled (ZFC) and field-cooled (FC) magnetization vs temperature curves. (a) $H=50$ Oe, (b) $H=5000$ Oe, and (c) $H=50$ kOe. Freezing temperatures (T_F) are indicated with arrows.

magnetic moment cannot be explained by this assumption. Second, a non-negligible content of Mn^{2+} would lead to an increase of the Curie constant, but we have mentioned that this situation is not structurally favored. Finally, some contribution to the effective magnetic moment could arise from itinerant electrons.[22] There are important experimental evidences that such kind of mechanism may play an important role in the measured enhancement of the magnetic moment. In fact, appreciable departures of the effective Curie constant from the expected value have been observed in another perovskite systems: it is reduced[22] in $SrFeMoO_6$, and enhanced[4] in $La_{0.67-x}Y_xCa_{0.33}MnO_3$. Since yttrium is always in the $3+$ state, the last compounds are expected to be a mixture of 67% Mn^{3+} and 33% Mn^{4+}. The measured value[4] of $C=2.95$ emu K/mole Oe is 12% higher than the calculated Curie constant. A similar deviation is found here for $La_{0.47}Ce_{0.20}Ca_{0.33}MnO_3$, with a difference of 18% between calculated and experimental values.

C. Low-temperature magnetization

The temperature dependence of the magnetization in the range 5–300 K is shown in Fig. 4. We measured the zero-field-cooled (ZFC) and field-cooled (FC) magnetization curves up to 300 K, for $H=50$ Oe, 5000 Oe, and 50 kOe. From the 50 Oe curves (see Fig. 4a), three temperature regimes can be defined according to the behavior observed in the ZFC and FC measurements: (i) From 5 to 70 K, there is a strong dependence on the magnetic history; (ii) between 70 and 200 K, some irreversibility still persists; and (iii) above 200 K the curves are fully coincident within experimental uncertainty. When the magnetic field is increased above 1 kOe, ZFC and FC curves differ only at the lowest temperatures, as shown in Fig. 4(b) and 4(c). The maximum in the low field (50 Oe) ZFC magnetization and the plateau of the FC suggest a ''freezing'' of the spin system below the temperature $T_F \sim 70$ K. In this case, the small ratio $T_F/\Theta \approx 0.2$ is an indication of the large degree of magnetic frustration. Recall that T_C/Θ (where T_C is the temperature of long-range ferromagnetic order) has been used in the same spirit to analyze the frustrated compounds $La_{0.67-x}Y_xCa_{0.33}MnO_3$ in Ref. 4.

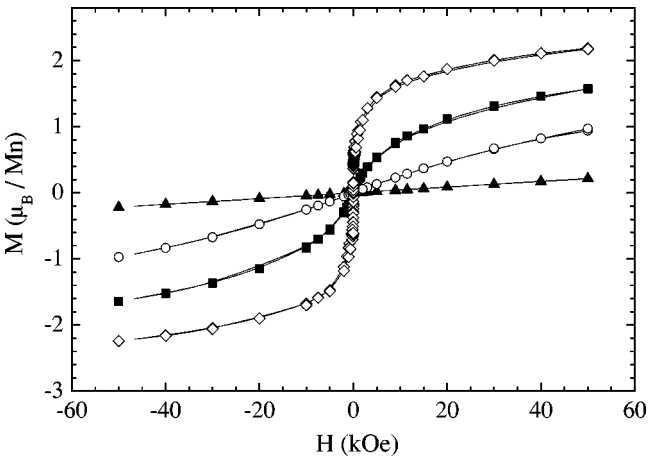

FIG. 5. Magnetization loops, measured at $T=5$ K (diamonds), 100 K (squares), 150 K (circles), and 295 K (triangles).

Detailed measurements of the Mn-magnetization vs field, shown in Figs. 5 and 6, complete the description of the low-temperature magnetic behavior. In Fig. 5, the shape of the magnetization loops changes strongly with temperature. The

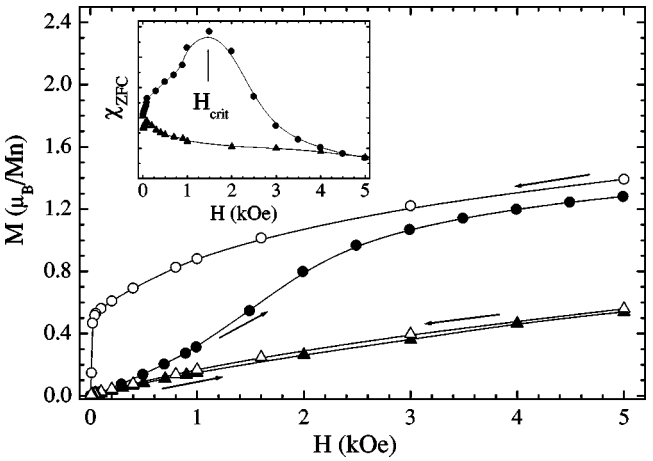

FIG. 6. Details of the magnetization curves, including the virgin branches (filled symbols), measured at 5 K (circles) and 100 K (triangles). The solid lines are guides to the eye. Inset: initial susceptibility, χ_{ZFC} vs H.

magnetization curve measured at 295 K indicates that the system is paramagnetic at high temperatures. In region (ii), the magnetization increases slowly with magnetic field in the whole H range. A small hysteresis arises below 200 K, and increases slowly as the temperature is decreased. A tiny coercive field $H_c < 20$ Oe is measured at 5 K, similar to those observed in $La_{0.67}Ca_{0.33}MnO_3$ compounds.[23] Due to the elongated shape of the magnetization loops, with very small remanence and coercivity,[24] it is very difficult to estimate the ferromagnetic (FM) fraction of the sample.

The magnetization does not saturate at low temperatures, even at 50 kOe, and attains $2.2\mu_B$/Mn at 50 kOe and 5 K, far below the Mn-system saturation value $M_{sat} \approx 3.79\mu_B$. This result is another indication of a highly frustrated spin system. In FM manganites, the magnetization usually saturates above $H \sim 2$ kOe. This is not the case of the lower temperature loops [region (i)], where $(M_i - M_d)/M(50\ \text{kOe}) = 2\%$ at 50 Oe, and the hysteresis closes at 5 kOe.

ZFC magnetization branches, measured below and above the freezing temperature $T_F \approx 70$ K, are shown in Fig. 6. At $T = 5$ K, the virgin curve exhibits an S-shaped form. The initial susceptibility $\chi_{ZFC} = [\partial M_{ZFC}/\partial H]_{H=0}$, is smaller than the susceptibility reached at an inflection point of M_{ZFC} for a critical field, H_{crit}. This behavior is better evidenced in the inset of Fig. 6, where χ_{ZFC} vs H is plotted. The maximum of χ_{ZFC} is observed at the critical field, $H_{crit} \approx 1490$ Oe. Above T_F, the S shape of the virgin curve is blurred and χ_{ZFC} has a small maximum at $H \approx 0$. This S behavior of the ZFC magnetization has been observed in a wide variety of spin-glasses below the freezing temperature,[25] and adds more evidence for the existence of a frustrated, glassy state in $La_{0.47}Ce_{0.20}Ca_{0.33}MnO_3$.

D. Resistivity and magnetoresistance

Figure 7(a) shows the temperature dependence of the resistivity $\rho(T)$, measured at zero field, and applying $H = 50$ kOe. The $La_{0.47}Ce_{0.20}Ca_{0.33}MnO_3$ samples are much more resistive than $La_{2/3}Ca_{1/3}MnO_3$: the RT resistivity of the former samples is three orders of magnitude higher.[26] This ratio is also found when comparing residual resistivities ρ_0 (measured at 4 K). At high temperature, T > 180 K, $\rho(T)$ shows a thermally activated behavior: $\rho(T) = \rho_\infty \exp(\Delta/k_B T)$. The activation energy deduced from the fits, $\Delta = 130$ meV, is higher than the values measured in $La_{2/3}Ca_{1/3}MnO_3$ compounds, $\Delta = 54$ meV.[26] This increase of the gap suggests that Ce doping not only modifies the scattering potential but it affects the band structure of the compound.

The zero-field resistivity has a maximum around $T_M \approx 145$ K, that signals the metal-insulator (M-I) transition, usually found in ferromagnetic manganite compounds. The relation $\rho(T_M)/\rho(20\ \text{K}) \sim 930$ is huge, much larger than the values found in $La_{0.67}Ca_{0.33}MnO_3$ compounds.[26–28] It must be noted that the parent compound $La_{0.67}Ca_{0.33}MnO_3$ presents the M-I transition at a higher temperature[26] ($T_M = 260$ K), close to the FM transition of the Mn moments. As we commented above, the magnetization curves of

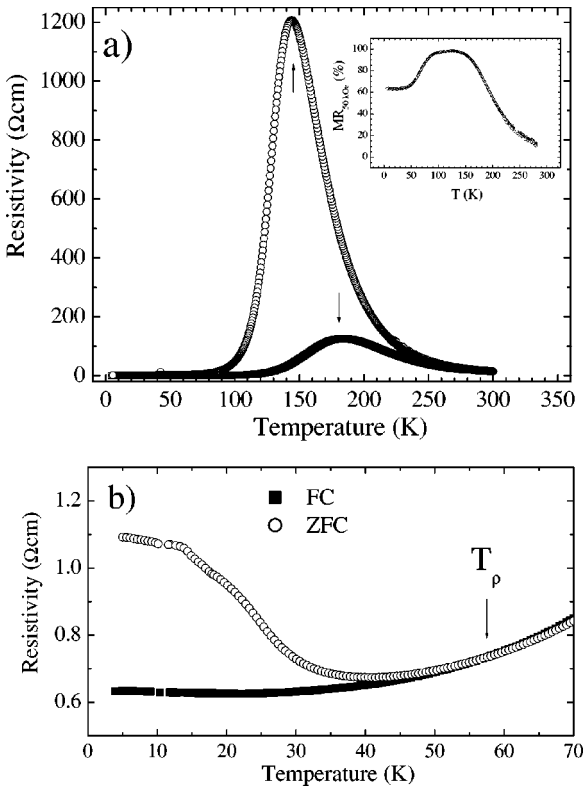

FIG. 7. (a) Resistivity vs temperature, measured at $H = 0$ (empty symbols) and $H = 50$ kOe (filled symbols). M-I transition temperatures (T_M) are indicated by arrows. Inset: T dependence of the MR, as obtained from data in (a). (b) ZFC and FC resistivity curves ($H = 20$ kOe).

$La_{0.47}Ce_{0.20}Ca_{0.33}MnO_3$ do not show clear evidences of a long-range order (LRO) magnetic transition. We have observed that there is a tiny hysteresis between ZFC and FC magnetization curves below 200 K, and the presence of FM short-range ordered (SRO) regions is evident from the magnetization loops measured in the same temperature range. The M-I transition may indicate the percolation of FM regions across the sample. It is known that the conduction electrons are driven in the lowest resistive channels. Therefore, our results can be explained by the existence of a short circuit through the percolated FM regions. Within this picture, the effect on the resistance of the presence of more disordered zones would be negligible. The shape of the magnetization loops does not allow one to estimate the FM fraction of the samples accurately. It is also known that the percolation limit strongly depends on the geometrical arrangement of the entities:[29] the theory of random continuum percolation gives a volume concentration limit as low as $x_p = 0.15$, while this concentration limit is raised to $x_p = 0.31$ for a three-dimensional cubic lattice. However, the relative proportion of ferromagnetic phase (short- and long-range order) may be rather small. Studies performed in Au-Fe and Cu-Ni alloys determined a percolation of a LRO zone[30] for a magnetic concentration of around 15%.

At low temperature ($T \sim 20$ K) a resistivity minima is measured. This feature has been recently attributed to electron-electron quantum interference,[31] usually found in

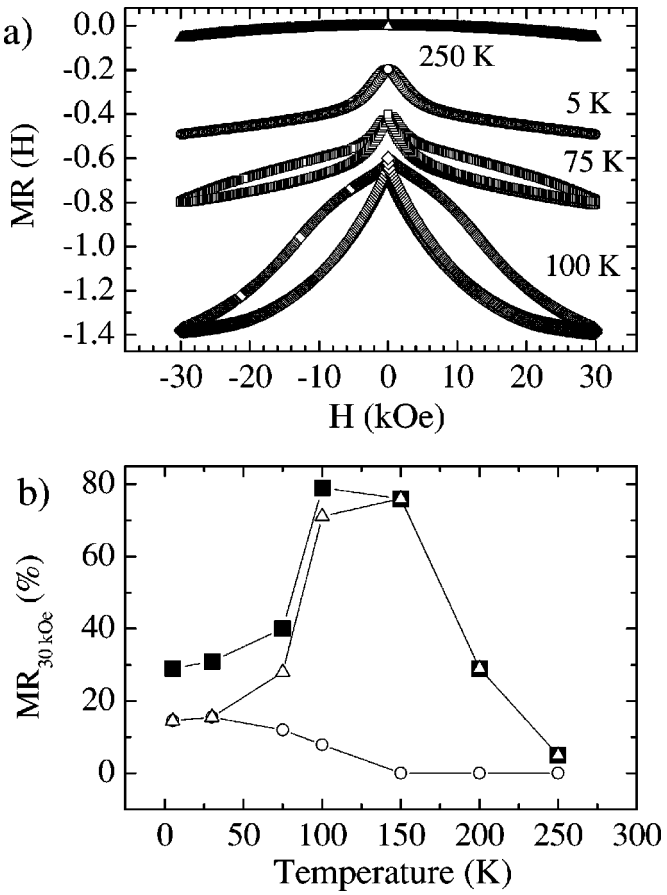

FIG. 8. (a) Normalized magnetoresistance $MR(H)=[R(H)-R(0)]/R(0)$ vs field, for $T=5$ K (circles), 75 K (squares), 100 K (diamonds), and 250 K (triangles). The $T=75$, 150, and 5 K curves have been displaced by -0.20, -0.40, and -0.60, respectively. (b) Total MR (filled squares), LFMR (circles), and IMR (triangles) components of the magnetoresistance, as deduced from data in (a).

disorder alloys. Similar behaviors have been also reported for spin glasses and distorted bulk $La_{0.67-x}Y_{0.20}Ca_{0.33}MnO_3$, being associated with different physical phenomena.[32] Further experiments are needed to elucidate the origin of these results.

The resistivity has also been measured under ZFC and FC conditions, with a measurement field of 20 kOe. We looked for magnetohistory effects, associated with the frustrated magnetic phase observed in the magnetization curves at low temperature. An enlarged view of the low-temperature region of these curves is shown in Fig. 7(b). The FC resistivity remains smaller than the ZFC resistivity below a characteristic temperature $T_\rho \approx 60$ K. These results show the influence of the whole magnetic structure on the charge carriers. In fact, the described behavior can be ascribed to spin-dependent scattering mechanisms present in the magnetically frustrated system.

The resistivity measured under an applied field of 50 kOe drops several orders of magnitude and presents a maximum at higher temperatures, confirming the direct correlation between spin disorder and the *M-I* transition. The temperature dependence of the magnetoresistance ratio MR (50 kOe) $\equiv 100*[R(0)-R(50\ \text{kOe})]/R(0)$, is plotted in the inset of Fig. 7. It reaches a flat maximum close to 100% between 100 and 150 K.

Normalized magnetoresistance loops $MR(H)\equiv[R(H)-R(0)]/R(0)$, measured at different temperatures between 5 K and 300 K, are presented in Fig. 8(a). Here also, as in the case of magnetization data, three different temperature regimes can be identified, according to the shape of the curves. For $T<75$ *K* [region (i)], the curves measured under increasing and decreasing magnetic fields, are almost completely reversible and exhibit an important low field magnetoresistance (LFMR).[33] The LFMR fraction is determined from the $MR(H)$ curves [Fig. 8(a)]. It is calculated as the ratio $\Delta R/\Delta R_{total}=100*[R(H=0)-R(H_{max})]/[R(H=0)-R(H=30\ \text{kOe})]$, being H_{max} the magnetic field where a change of slope is measured in the low-field region of the curve. This feature is particularly noticeable in the lowest temperature plots, i.e., $T=5$ and 75 K. The intrinsic magnetoresistance (IMR) fraction is obtained by difference between the total MR and the LFMR.

The LFMR component is attributed to spin-dependent intergrain scattering, and increases with decreasing temperature due to the progressive increase of the spin polarization of the carriers. A non-negligible quasilinear decrease of the resistivity is observed at higher fields. This magnetoresistance component is intrinsic (IMR), and has been traditionally explained in manganites by the double exchange coupling[1] between Mn^{3+} and Mn^{4+} ions. In the $75\ \text{K} \leqslant T \leqslant 200$ K range [region (ii)], the $\rho(H)$ curves are characterized by a strong hysteresis. The irreversibility increases abruptly above 60 K, passes through a maximum at $T\sim 100$ K, and decreases smoothly, attaining zero above 200 K. The $MR(H)$ curves have been measured in different magnetic field sweep rates between 1 and 6 kOe/min, without finding any change in the hysteresis of the curves, meaning that the relaxation processes involved in this effect are very slow and of characteristic times much different from the measuring times. For $T\geqslant 200$ K [region (iii)], the MR is very small, decreasing smoothly with increasing temperature, and the curves show no hysteresis. They have a bell-shape found in FM manganites above T_C.[33]

The temperature dependence of the low-field and high-field magnetoresistance contributions, estimated from the $MR(H)$ curves, are plotted in Fig. 8(b). We observe that the total magnetoresistance, as well as the LFMR and IMR components, remain constant below T_F. The simultaneous ''freezing'' of both the extrinsic and intrinsic magnetoresistance at around 30% is unusual in manganite systems, and it is probably associated with the low-temperature glassy phase.

IV. CONCLUSIONS

We have obtained single-phase, high-quality polycrystalline samples using the nitrate decomposition route. XPS measurements on $La_{0.47}Ce_{0.20}Ca_{0.33}MnO_3$ indicate that both $3+$ and $4+$ charge states of cerium ions are present in an estimated 40–60 % relation, giving a compound with an effective hole doping level of 21%.

The low ratio $T_F/\Theta \approx 0.2$ observed in the high-temperature susceptibility, together with the low-T magnetization measurements, indicates that $La_{0.47}Ce_{0.20}Ca_{0.33}MnO_3$ orders in a complex magnetic structure, built of ferromagnetic SRO regions with a broad size distribution, either embedded in a frustrated matrix or coupled forming a cluster-glass system. This behavior could be understood in the frame of intrinsic cation disorder and consequent structural distortions. As occurs in $La_{0.67}Y_xCa_{0.33}MnO_3$ compounds,[4] magnetic frustration would arise in $La_{0.47}Ce_{0.20}Ca_{0.33}MnO_3$ from the competing FM (double exchange) and antiferromagnetic (superexchange) interactions in a background of structural disorder. In $La_{0.47}Ce_{0.20}Ca_{0.33}MnO_3$, the disorder arising from the La substitution and the random positions of Mn^{3+} and Mn^{4+} ions, is reinforced by the presence of cerium ions in the $3+$ and $4+$ charge states.

A metal-insulator transition is observed at $T_M \approx 145$ K that moves to higher temperature when a magnetic field is applied. This fact, together with the large magnetoresistance ratios observed, reveals the magnetic nature of the M-I transition in a system where long-range FM order is not evident to set up. This is a very interesting feature of $La_{0.47}Ce_{0.20}Ca_{0.33}MnO_3$ that suggests the existence of a low-lying, FM short-range order that would play a crucial role in the transport properties. The M-I transition is associated with a percolation of the FM regions across the sample, and is explained by DE interactions between Mn^{3+} and Mn^{4+} ions. The large MR ratios could be explained within the same picture. However, the anomalous low-T dependence of the magnetoresistance, and the magnetic-history-dependent behavior of the resistivity, can only be explained by the introduction of other sources of spin-dependent scattering, related to the low-temperature, glassy phase of the system.

A clear correlation between magnetic and transport properties has been found in the whole temperature range. In fact, the magnetic behavior of the system is reflected in the resistivity measurements.

ACKNOWLEDGMENTS

We thank Adriana Serquis, Marcelo Vázquez Mansilla and Martín Sirena for experimental assistance, and Rorberto Zysler for useful discussions. We acknowledge support from FOMEC program, CONICET (PIP 4947), ANPCYT (PICT 3-52-1027 and 3-6340), and Fundación Antorchas, Argentina. M.T., L.B. S., D.G.L., G.Z., G.A., and J.E.G. are members of CONICET.

*Corresponding author: Email address: galejand@cab.cnea.gov.ar
†Present address: Institute for Storage Ring Facilities, University of Aarhus, DK-8000 Aarhus C, Denmark
‡Present address: Sincrotrone Trieste S.C.p.A., S.S.14 Km 163.5, 34012 Trieste, Italy

[1] C. Zener, Phys. Rev. **82**, 403 (1951); P.W. Anderson and H. Hasegawa, *ibid.* **100**, 675 (1955).
[2] J.L. García-Muñoz, J. Fontcuberta, B. Martínez, A. Seffar, S. Piñol, and X. Obradors, Phys. Rev. B **55**, 668 (1997); B. Martínez, J. Fontcuberta, A. Seffar, J.L. García-Muñoz, S. Piñol, and X. Obradors, *ibid.* **54**, 10 001 (1996).
[3] J. Fontcuberta, B. Martínez, A. Seffar, S. Piñol, J.L. García-Muñoz, and X. Obradors, Phys. Rev. Lett. **76**, 1122 (1996).
[4] G. Alejandro, M.T. Causa, M. Tovar, J. Fontcuberta, and X. Obradors, J. Appl. Phys. **87**, 5603 (2000).
[5] J.M. de Teresa, M.R. Ibarra, J. García, J. Blasco, C. Ritter, P.A. Algarabel, C. Marquina, and A. del Moral, Phys. Lett. **76**, 3392 (1996).
[6] M. Uehara, S. Mori, C.H. Chen, and S.W. Cheong, Nature (London) **399**, 560 (1999).
[7] J. Philip and T.R. Kutty, J. Phys.: Condens. Matter **11**, 8537 (1999).
[8] P. Mandal and S. Das, Phys. Rev. B **56**, 15 073 (1997).
[9] P. Raychaudhuri, S. Mukherji, A.K. Nigam, J. John, U.D. Vaisna, and R. Pinto, J. Appl. Phys. **86**, 5718 (1999).
[10] J.R. Gebhardt, S. Roy, and N. Alí, J. Appl. Phys. **85**, 5390 (1999).
[11] J.S. Kang, Y.J. Kim, B.W. Lee, C.G. Olson, and B.I. Min, J. Phys.: Condens. Matter **13**, 3779 (2001).
[12] J. Rodríguez Carvajal, Physica B **192**, 55 (1993).
[13] R. Ganguly, I.K. Gopalakrishnan, and J.V. Yakhmi, J. Phys.: Condens. Matter **12**, L719 (2000).
[14] H.Y. Hwang, S.W. Cheong, P.G. Radaelli, M. Marezio, and B. Batlogg, Phys. Rev. Lett. **75**, 914 (1995).
[15] J.M.D. Coey, M. Viret, and S. von Molnár, Adv. Phys. **48**, 167 (1999).
[16] J.L. García-Muñoz, M. Suaaidi, J. Fontcuberta, and J. Rodríguez-Carvajal, Phys. Rev. B **55**, 34 (1997).
[17] Q. Huang, A. Santoro, J.W. Lynn, R.W. Erwin, J.A. Borchers, J.L. Peng, and R.L. Greene, Phys. Rev. B **55**, 14 987 (1997).
[18] D.R. Mullins, S.H. Overbury, and D.R. Huntley, Surf. Sci. **409**, 307 (1998).
[19] S.Y. Wu, C.C. Yang, W.H. Li, K.C. Lee, J.W. Lynn, and H.D. Yang, J. Magn. Magn. Mater. **239**, 14 (2002).
[20] M.T. Causa, M. Tovar, A. Caneiro, F. Prado, G. Ibáñez, C.A. Ramos, A. Butera, B. Alascio, X. Obradors, S. Piñol, F. Rivadulla, C. Vázquez-Vázquez, A. López-Quintela, J. Rivas, Y. Tokura, and S.B. Oseroff, Phys. Rev. B **58**, 3233 (1998).
[21] M. Tovar, G. Alejandro, A. Butera, A. Caneiro, M.T. Causa, F. Prado, and R.D. Sánchez, Phys. Rev. B **60**, 10 199 (1999).
[22] M. Tovar, M.T. Causa, A. Butera, J. Navarro, B. Martínez, J. Fontcuberta, and M.C.G. Passeggi, Phys. Rev. B **66**, 024409 (2002).
[23] G.J. Snyder, R. Hiskes, S. DiCarolis, M.R. Beasley, and T.H. Geballe, Phys. Rev. B **53**, 14 434 (1996).
[24] F. Prado, R.D. Sánchez, A. Caneiro, M.T. Causa, and M. Tovar, J. Solid State Chem. **146**, 418 (1999).
[25] K. Binder and A. P. Young, Rev. Mod. Phys. **58**, 818 (1986), and references therein.
[26] A.K.M. Akther Hossain, L.F. Cohen, F. Damay, A. Berenov, J. Mac Manus-Driscoll, N.McN. Alford, N.D. Mathur, M.G. Blamire, and J.E. Evetts, J. Magn. Magn. Mater. **192**, 263 (1999).
[27] J.M. De Teresa, M.R. Ibarra, J. Blasco, J. García, C. Marquina, P.A. Algarabel, Z. Arnold, K. Kamenev, C. Ritter, and R. von Helmolt, Phys. Rev. B **54**, 1187 (1996).

[28] S.H. Park, Y-H. Jeong, K-B. Lee, and S.J. Kwon, Phys. Rev. B **56**, 67 (1997).
[29] A. Butera, T.J. Klemmer, and J.A. Barnard, J. Appl. Phys. **83**, 4855 (1998).
[30] D. Stanffer, in *Amorphous Magnetism*, edited by R. Levy and B. Hasegawa (Premium Press, New York, 1997), Vol. 2.
[31] D. Kumar, J. Sankar, J. Narayan, R.K. Singh, and A.K. Majumdar, Phys. Rev. B **65**, 094407 (2002).
[32] P. L. Rossiter, *The Electrical Resistivity of Metals and Alloys*, Cambridge Solid State Science Series (Cambridge University Press, Cambridge, 1987).
[33] H.Y. Hwang, S.W. Cheong, N.P. Ong, and B. Batlogg, Phys. Rev. Lett. **77**, 2041 (1996).